energies

MDPI

Article

Thermochemical Characterizations of Novel Vermiculite-LiCl Composite Sorbents for Low-Temperature Heat Storage

Yannan Zhang, Ruzhu Wang *, Tingxian Li and Yanjie Zhao

Institute of Refrigeration and Cryogenics and Key Laboratory of Power Mechanical Engineering, Ministry of Education of The People's Republic of China, Shanghai Jiao Tong University, Shanghai 200240, China; zyn1126@sjtu.edu.cn (Y.Z.); litx@sjtu.edu.cn (T.L.); zhaoyanjie@sjtu.edu.cn (Y.Z.)

* Correspondence: rzwang@sjtu.edu.cn; Tel.: +86-21-3420-6548

Academic Editor: Maurizio Sasso

Received: 27 June 2016; Accepted: 10 October 2016; Published: 22 October 2016

Abstract: To store low-temperature heat below 100 °C, novel composite sorbents were developed by impregnating LiCl into expanded vermiculite (EVM) in this study. Five kinds of composite sorbents were prepared using different salt concentrations, and the optimal sorbent for application was selected by comparing both the sorption characteristics and energy storage density. Textural properties of composite sorbents were obtained by extreme-resolution field emission scanning electron microscopy (ER-SEM) and an automatic mercury porosimeter. After excluding two composite sorbents which would possibly exhibit solution leakage in practical thermal energy storage (TES) system, thermochemical characterizations were implemented through simulative sorption experiments at 30 °C and 60% RH. Analyses of thermogravimetric analysis/differential scanning calorimetry (TGA/DSC) curves indicate that water uptake of EVM/LiCl composite sorbents is divided into three parts: physical adsorption of EVM, chemical adsorption of LiCl crystal, and liquid–gas absorption of LiCl solution. Energy storage potential was evaluated by theoretical calculation based on TGA/DSC curves. Overall, EVMLiCl20 was selected as the optimal composite sorbent with water uptake of 1.41 g/g, mass energy storage density of 1.21 kWh/kg, and volume energy storage density of 171.61 kWh/m^3.

Keywords: sorbent; expanded vermiculite (EVM); lithium chloride; solution carryover; thermal energy storage (TES)

1. Introduction

Solar energy is regarded as a promising alternative to traditional energy resources, and the potential usage in residency and industry has been widely researched. However, its practical utilization is hindered by the mismatch between energy supply and demand. As an emerging technology, thermal energy storage (TES) is an efficient method to realize sustainable usage of solar energy [1]. Methods of TES are mainly divided into three types: latent heat storage, sensible heat storage, and thermochemical heat storage. Although latent heat storage and sensible heat storage have been widely investigated in recent decades, insufficient studies on thermochemical heat storage have been carried out, which is also competitive and attracting burgeoning interests owing to higher energy storage density and negligible heat loss over a long-term storage period.

Increasing studies [2–7] have adopted water as sorbate for its safety and low price. Water sorption materials can be generally divided into three types: physical sorbents such as silica gel and zeolite; chemical sorbents represented by LiCl and $MgCl_2$; and composite sorbents, also called "salt inside porous matrix (CSPM)". In this study, CSPM was selected as the water sorption material. The hydration

reaction of hydroscopic salts can release a relatively enormous amount of heat compared to physical sorption of porous matrixes. However, the use of bulk hydroscopic salt comes with the problems of solution carryover, swelling, and agglomeration, which lead to sharp decrease of actual released heat, serious unreliability, and nonrepeatability. CSPM is the composite of two components: hydroscopic salt and host matrix. In host matrix, salt molecules are dispersed in the pores and crystalize on the surface of interlayers. Instead of compact aggregation, which commonly appears in bulk material, salt crystals are separated in the form of small-scale particle aggregations. As a consequence, the contact areas between salt crystals and water vapor are extensively raised, which enhances the mass transfer and thus promotes sorption kinetics. The phenomena of swelling and agglomeration are also markedly decreased. Besides, the pores may potentially provide volume for salt solution formed in sorption process.

Although CSPM represents excellent performance in avoiding both swelling and agglomeration and improving mass transfer, effective control of solution leakage remains a major problem to be solved. Both the sorption phases and capacity of water uptake are controlled by temperature and relative humidity (RH). Hydroscopic salts begin to adsorb water vapor when RH exceeds the equilibrium humidity of hydration reaction and hydrous salts are formed. Furthermore, if RH exceeds the deliquescence relative humidity (DRH), the formed hydrous salts continue to absorb water vapor and salt solution, and eventually appear due to deliquescence. To obtain large water uptake, highly hydrophilic salts, such as LiCl, are generally chosen as an impregnant in CSPM. The DRH of such hydrophilic salts is relatively low (11% RH at 30 °C), thus the deliquescence phenomenon should appear in a practical TES system. Several previous studies have proposed some methods to prevent solution leakage of CSPM. Gong et al. [8] eliminated the possibility of solution leakage of silica gel-LiCl sorbents by putting newly synthesized samples on a strainer in a constant-temperature and constant -humidity chamber at 30 °C and 90% RH to remove the leaked solution. Yu et al. [9] selected the optimal silica gel-LiCl sorbent by comparing the full water uptake in different working conditions with related pore volume, and the largest isobaric water uptake of the best-performing candidate without solution leakage is around 0.6 g/g at 1.66 kPa. In their studies, despite preventing solution leakage, water uptake was confined to a limited amount.

It is of great significance to avoid solution leakage on the prerequisite of utilizing the extra water uptake introduced by salt deliquescence as much as possible. The vital point lies in choosing appropriate porous matrix material which has enough pore volume as well as sufficient holding-strength for confining the solution in the pores. Silica gel and zeolite are conventional porous host matrixes applied to developing CSPM. The pore volume of silica gel is usually smaller than 1.0 cm^3/g [10]. Pore volume of zeolite is even smaller than that of silica gel, ranging from 0.01 to 0.32 cm^3/g [11]. In other words, assuming all the pore spaces are occupied by salt solution, the largest water uptake which can be received by silica gel and zeolite is lower than 1.0 g/g and 0.32 g/g, respectively. Generally, to improve the water uptake of CSPM, a novel porous host matrix with much larger pore volumes is necessary to be employed. In this study, expanded vermiculite (EVM) was chosen as the host matrix, which has a macrospore structure with pore volume varying from 2.8 to 4.1 cm^3/g and average pore diameter of 600–3680 nm [12,13]. This structure contributes to a great potential for water uptake. Besides, EVM also enjoys obvious merits such as nontoxicity and low-cost. However, limited studies have employed EVM for developing composite water sorbents for TES application. Aristov et al. [14] developed a water sorbent based on expanded vermiculite as a host matrix and calcium chloride as a hygroscopic salt. They found that formation of $CaCl_2$ solution may occur without overflow a large amount of water uptake. Shkatulov et al. [15] proposed a new $Mg(OH)_2$/vermiculite composite material for middle-temperature heat storage. Sapienza [16] presented a new composite water sorbent $LiNO_3$/vermiculite for adsorption chilling at low temperature (<70 °C). Other studies of EVM for TES application are mainly focused on ammonia adsorption [17,18] and developing phase change materials (PCMs) [19,20].

The purpose of this study is to develop and optimize novel CSPMs with high-energy storage density for TES below 100 °C. EVM was chosen as the host matrix based on the reasons described above. LiCl was selected as the salts embedded into EVM, since its excellent energy storage performance has been proved in previous studies such as references [21–23]. EVM/LiCl composite sorbents with different salt contents were developed by impregnation at atmospheric temperature and pressure. To identify the threshold salt content for solution leakage, simulative sorption experiments were carried out in a constant temperature and humidity chamber. Composite sorbents which conquer with the phenomenon of solution leakage were excluded. Pore structure of composite sorbents was observed and analyzed by ER-SEM and automatic mercury porosimeter. Compared with bulk LiCl crystals, the changes in sorption kinetics and sorption equilibrium caused by pore structure of EVM were analyzed. Simultaneous thermal analysis experiments and theoretical calculation based on thermogravimetric analysis/differential scanning calorimetry (TGA/DSC) curves were conducted to explore water uptake behavior and to assess the energy storage potential of EVM/LiCl composite sorbents. Accordingly, optimal composite sorbents were selected.

2. Experimental

2.1. Development and Preliminary Selection of Materials

The EVMs employed in this study have a particle size of 5–8 mm. The fabrication of composite desiccant materials was as follows. First, EVMs were pretreated by complete drying at 200 °C for 4 h. Then the dried EVMs were immersed into LiCl solution with different concentrations of 5%, 10%, 20%, 30%, and 40%, respectively, for 48 h, which can ensure the thorough impregnation of LiCl solution into pores. After that, a sieve was utilized to separate the wet sorbents from solution. LiCl solution attached on the EVM surface was removed by quick washing using distilled water. Finally, wet sorbents were dried in the oven at 120 °C until the total mass remained constant. Composite sorbents with five different salt contents were synthesized, and they were consequently named as EVMLiCl5, EVMLiCl10, EVMLiCl20, EVMLiCl30, and EVMLiCl40 with respect to the mass concentrations of LiCl solution.

Preliminary selection was conducted by simulative sorption experiments in a constant temperature and humidity chamber, aiming at excluding composite sorbents which suffer from solution leakage under TES working conditions. In a practical closed TES system, the sorption temperature is higher than 30 °C while the evaporation temperature is lower than 20 °C. Thus the largest water uptake is obtained at the condition of 30 °C and 60% RH (water vapor pressure under this condition equals saturated water vapor pressure at 20 °C). The testing condition of the constant temperature and humidity chamber was set at 30 °C and 60% RH, and EVM and EVM/LiCl sorbents which were fully predried at 120 °C were put in. They were weighted every 30 min until sorption equilibrium is reached. After the first experiment, solution leakage appeared on EVMLiCl20, EVMLiCl30, and EVMLiCl40. The leaked solution of EVMLiCl20 was adsorbed by blotting paper and then the sorbents were fully dried in an oven. By exactly weighing the mass of newly obtained EVMLiCl20, the new salt content in sorbents could be identified. A secondary simulative sorption experiment on this new EVMLiCl20 from the first experiment showed no solution leakage, indicating a convincing salt concentration threshold (32.60%). This threshold also implies no necessity for further study on LiCl30 and LiCl40. Therefore, EVMLiCl5, EVMLiCl10, and EVMLiCl20, given deliquescence treatments which were free from solution leakage, were chosen as promising candidates to apply in TES system, and their application potentials were further studied as described below. The salt content and bulk density of EVM and adopted composite sorbents are shown in Table 1.

Table 1. The salt concentration and bulk density of sorbents.

	Sample	EVM	EVMLiCl5	EVMLiCl10	EVMLiCl20
Before deliquescence	Salt content [1] (wt %)	0.00	11.89	23.74	34.30
	Bulk density [2] (kg/m^3)	127.74	130.00	133.71	143.91
After deliquescence	Salt content (wt %)	/	11.89	23.74	32.60
	Bulk density (kg/m^3)	/	130.00	133.71	141.50

[1] Meaning the mass ratio of LiCl; [2] The bulk density was obtained by measuring the volume of particular mass of sorbents at natural bulk state.

2.2. Characterization Methods

Microstructure and salt distribution on the surface of EVM were obtained by extreme-resolution field emission scanning electron microscopy (ER-SEM, JEOL JSM-7800F Prime, JEOL Ltd., Tokyo, Japan). High-resolution observation on low-electrical conductivity can be achieved with a maximum magnification of 10^6.

Macrospore structure including pore volume, pore size, and pore area were measured by automatic mercury porosimeter (AutoPore IV 9510, Micromeritics Instrument Corp., Atlanta, GA, USA). The measurable pore size range is from 30 to 3600 nm.

Simulative sorption experiment and sorption kinetics measurement were implemented in a constant-temperature and -humidity chamber (Binder KMF115, Suzhou Baizhao Scientific Instrument Ltd., Suzhou, China). The temperature and relative humidity accuracy is ±0.1 °C and ±2.0%, respectively. Before the test, samples (except pure LiCl crystals) were fully dried at 120 °C. Then, after the condition of temperature and humidity chamber reached the defined condition, they were put into the chamber and weighed every 30 min using an electronic balance whose accuracy is 0.001 g.

Thermochemical measurements were conducted in simultaneous thermal analyzer (Netzsch STA 449 F3, Netzsch, Shanghai, China). Variation of mass and heat flow under increasing temperature were recorded simultaneously. The resolutions of weight measurement and heat-flow measurement are 0.1 μg and 1 μW respectively. The instrument was calibrated before the tests. In this study, about 10 mg sorbent was put into the simultaneous thermal analyzer (STA) instrument after simulative sorption experiment and was heated from room temperature up to 250 °C with increments of 5 °C/min. During the test period, desorption occurred and related data was collected.

3. Results and Discussion

3.1. Textural Properties

Figure 1 shows the ER-SEM images of EVM, EVMLiCl10, and EVMLiCl20. As seen in Figure 1a, the pores in EVM are formed by the stacking of numerous layers, and irregular shapes are presented. In Figure 1b,c, the small white spots represent the aggregates of LiCl crystals. It is shown that LiCl crystals distributed separately on the surface of the EVM layers. The regularity of distribution is influenced by morphology and roughness of the layers. Typically, with larger salt content, more salt crystals are observed on EVMLiCl20. Figure 1d is 25 times magnified image of the red circle in Figure 1c, which represents the aggregation state of LiCl crystals adhered to the surface of pores inside EVM. It can be seen that the LiCl crystals array orderly on the surface of the layer.

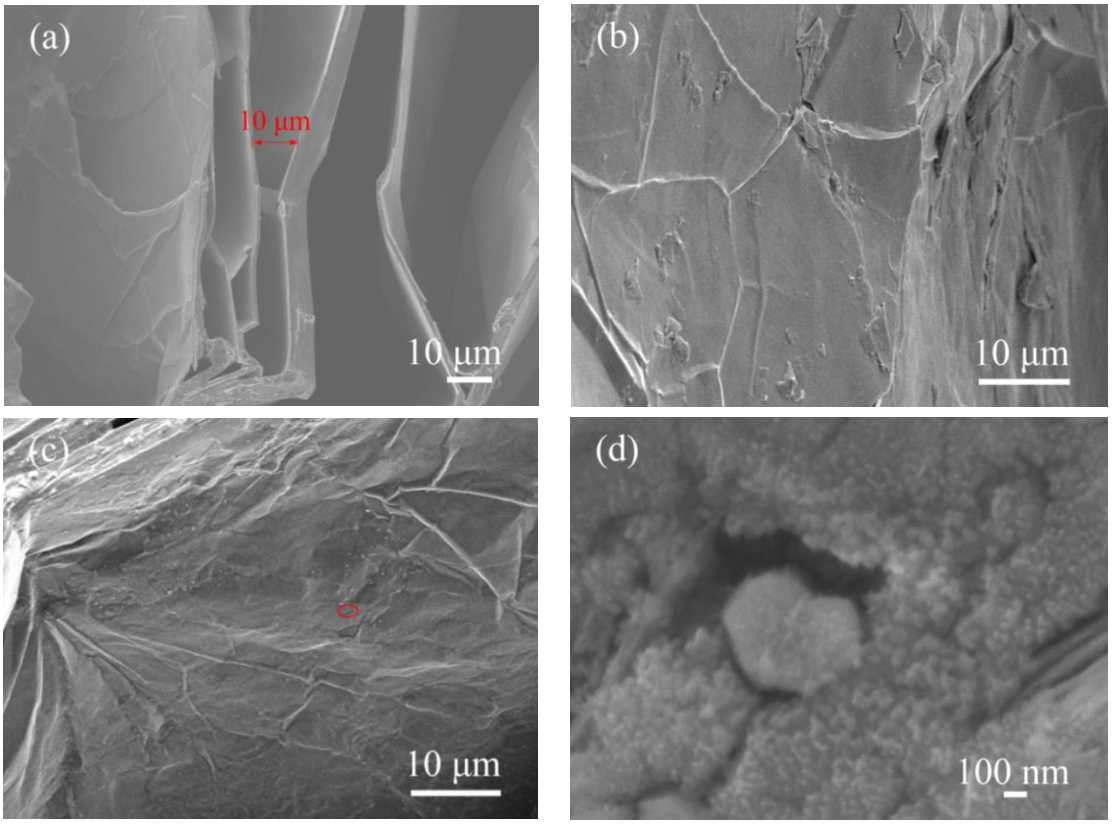

Figure 1. Extreme-resolution field emission scanning electron microscopy (ER-SEM) pictures of (**a**) expanded vermiculite (EVM); (**b**) EVM impregnated with 10% LiCl (EVMLiCl10); (**c**) EVMLiCl20; (**d**) LiCl crystal.

Pore structure parameters of EVM and EVM/LiCl composite sorbents are shown in Table 2. The pore volume of pure EVM is 4.7626 cm^3/g. When impregnating LiCl into pores of EVM, a decreased pore volume is induced by three major cases: (1) part of open pores is blocked by LiCl crystals; (2) newly closed pores are created by the stacking of LiCl crystals; (3) other parts of the volume are occupied by LiCl crystals. As seen in Table 2, the pore volume which is related to the EVM mass of composite sorbents is almost constant, slightly ranging from 2.6 to 2.9 cm^3/g, which is 0.55–0.62 times smaller than that of pure EVM. As the volume of LiCl crystals is lower than 0.3 cm^3/g, this decrease of pore volume is mainly ascribed to reasons (1) and (2) described above. Corresponding to the decrease of pore volume, the pore area oppositely increases from 2.623 to 3.121 m^2/g. Pore diameter lies in the range of 7300–8000 nm, and its connection/relation to salt content is weak.

Table 2. Pore parameters of EVM and EVM/LiCl composite sorbents.

Sample	EVM	EVMLiCl5	EVMLiCl10	EVMLiCl20
Salt content (wt %)	0.0	11.9	23.7	32.6
Pore volume (cm^3/g)	4.7626	2.3179	2.2099	1.9646
Volume of LiCl crystals (cm^3/g)	0	0.067	0.133	0.183
Pore volume (cm^3/g, related to the mass of pure EVM)	4.7626	2.8977	2.9147	2.6307
Volume of LiCl crystal [3] (cm^3, related to the mass of pure EVM)	0	0.076	0.175	0.272
Pore area (m^2/g)	0.671	2.623	2.744	3.121
Pore diameter (nm)	7663.4	7939.4	7363.8	7364.5

[3] Calculated based on salt content and true density of LiCl crystals.

3.2. Sorption Kinetics

Figure 2 shows the sorption kinetics of pure EVM, bulk LiCl crystals, and EVM/LiCl sorbents at 30 °C and 60% RH. Physical sorption rate of EVM is extremely fast, but the equilibrium value is only 0.04 g/g, which is ascribed to its macrospore structure. Capillary condensation of water vapor hardly happens in pores whose size are larger than 50 nm, thus the sorption performance of EVM is similar to that on ordinary flat, solid surface. For composite sorbents, mass transfer gets weaker with accumulating salt confined to pores in EVM, which requires more time to reach sorption equilibrium. Ninety-five percent of total water uptake of EVMLiCl5, EVMLiCl10, and EVMLiCl20 is reached in 90 min, 180 min, and 270 min, respectively. With enlarged salt content, the total water uptake increases from 0.49 g/g to 1.38 g/g. The sorption rate of pure LiCl is evidently lower than that of composite sorbents, and the sorption equilibrium is not reached until 690 min. This tremendous difference in equilibrium times verifies that sorption kinetics of LiCl is strengthened, which is attributed to the dispersed LiCl crystals in the pore structure of EVM. This porous structure in EVM provides vapor transport paths as well as heat transfer paths to LiCl crystals, and as a consequence sorption performance is promoted.

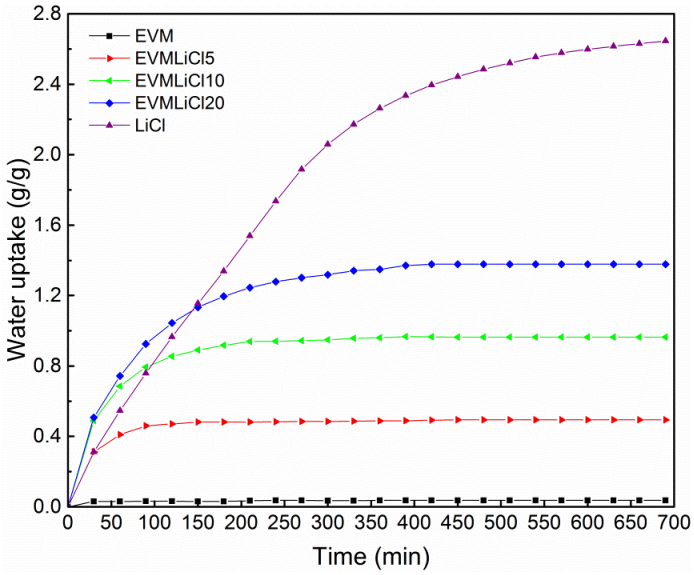

Figure 2. Water sorption kinetics of EVM, LiCl, and EVM/LiCl sorbents at 30 °C and 60% RH.

Due to the very poor sorption capacity of EVM, the vast majority of sorption process is caused by the reaction between LiCl and water vapor. The DRH of LiCl is only 11% at 30 °C, which guarantees the successful hydration reaction between LiCl and water vapor as well as liquid–gas absorption of LiCl solution where LiCl is finally dissolved in the solution at sorption equilibrium phase. According to the mechanics of salt solution absorption, absorption equilibrium is reached when saturated water vapor above aqueous solution of LiCl equals water vapor pressure of ambient air. Equilibrium mass concentration of LiCl solution is 23.7% at 30 °C and 60% RH based on the fitting formula summarized by Conde et al. [24], and the mass concentration is decided by temperature and water vapor pressure (which can be calculated from temperature and related humidity of moist air).

To evaluate the influence of EVM on absorption equilibrium of LiCl solution at 30 °C and 60% RH, mass concentration and volume of the LiCl solution formed in EVM pores are calculated by formulas below (assuming the sorption of EVM is not affected by LiCl and is related to its mass coefficients):

$$w = 100 \cdot \left(1 + \frac{x_{cs} - (1-\eta)x_{EVM}}{\eta}\right)^{-1} (\%) \quad (1)$$

$$v_s = \frac{1-\eta+\eta/w}{\rho_s} \ (cm^3/g\ sorbent) \tag{2}$$

where w is mass concentration of LiCl solution in EVM pores, η is salt content of composite sorbents, x_{cs} and x_{EVM} are corresponding equilibrium water uptake of composite sorbents and raw EVM respectively (obtained from Figure 2), v_s is the volume of LiCl solution, and ρ_s is the density of LiCl solution. The value of ρ_s is calculated by the simulation formula given by Conde et al. [24], and the value is in the function of temperature and mass concentration of LiCl solution.

Calculation results are shown in Figures 3 and 4. As seen from Figure 3, the mass concentration of LiCl solution generated in sorption process reveals a tenuous decreasing tendency with the increase of salt content in composite sorbents. While in the same condition, pure LiCl crystals without the restriction of a matrix achieve a 1.2 times higher mass concentration at equilibrium phase. This result demonstrates that sorption kinetics of LiCl crystals is enhanced when confined to host matrix pores.

Figure 4 shows the comparison of LiCl solution volume and related pore volume of three composite sorbents. Volume of formed LiCl solution increases from 0.5153 to 1.5220 cm^3/g with the increased salt content. EVMLiCl20 has a salt content threshold that can prevent solution leakage. However, it is noticed that solution volume of EVMLiCl20 is lower than total pore volume, which testifies that not all of the pore volume in EVM can be utilized. This can be explained from two aspects: on one hand, part of pore volume is blocked by salt solution and cannot be used as a result. On the other hand, the ability to hold solution is too weak to retain the solution close to the outside surface of EVM; this is due to the macrospores structures of EVM. In a word, the practical salt solution volume that EVM can hold is lower than its total pore volume.

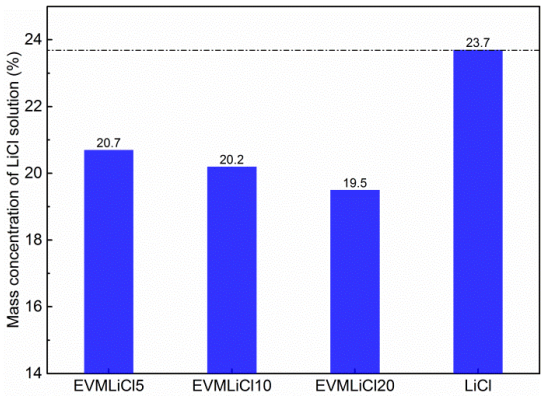

Figure 3. Comparison of mass concentration of formed LiCl solution of composite sorbents and bulk LiCl.

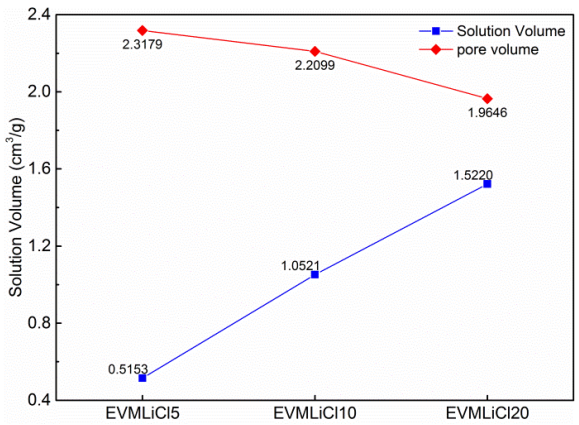

Figure 4. Total pore volume and LiCl solution volume filling in EVM pores of composite sorbents.

3.3. Thermal Characterizations Measurement

Results of STA measurements of EVM, LiCl, and EVM/LiCl composite sorbents are shown in Figure 5. The changes of mass and heat flow of sorbents as a function of temperature in the desorption process were simultaneously recorded, shown by the TGA curve (the blue line) and the DSC curve (the rose line), respectively.

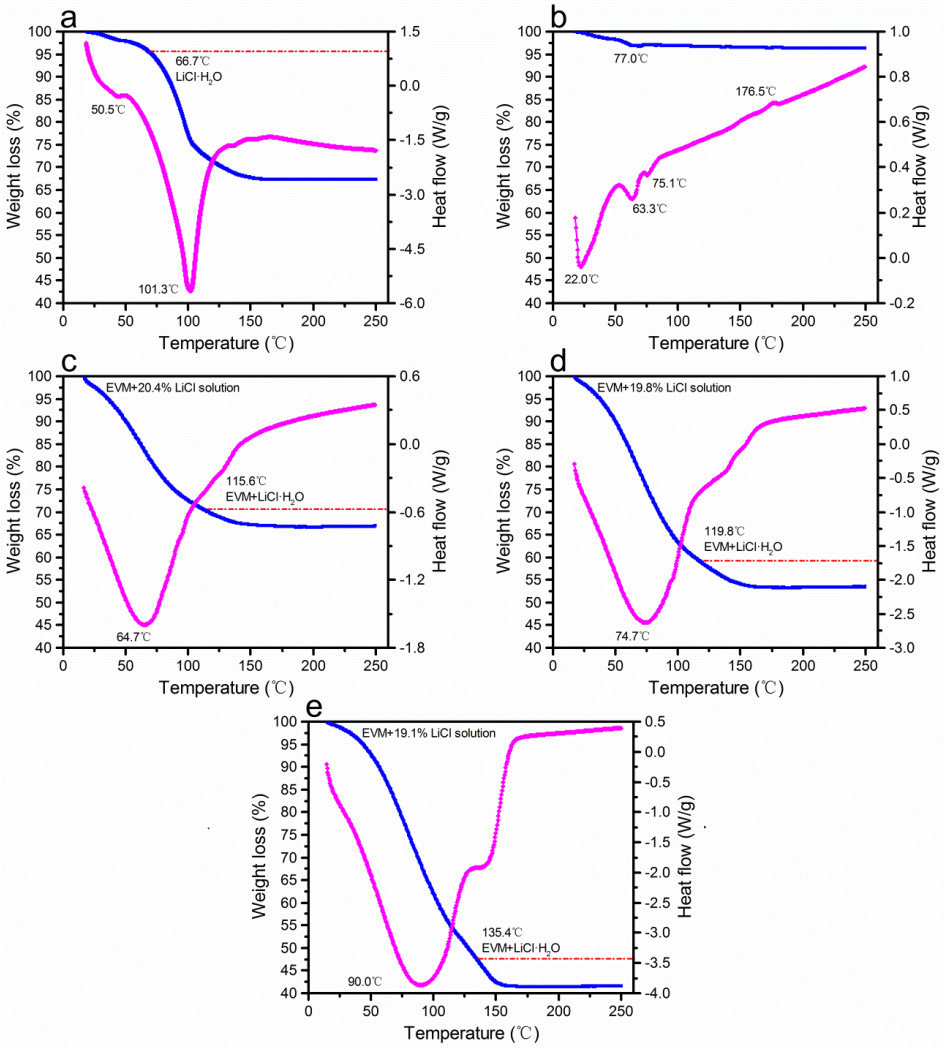

Figure 5. Results of simultaneous thermal analyzer (STA) measurement: (**a**) LiCl·H_2O; (**b**) EVM; (**c**) EVMLiCl5; (**d**) EVMLiCl10; (**e**) EVMLiCl20.

For EVM, the original water uptake is only 0.037 g/g. As seen in TGA curve, EVM loses almost all the adsorbed water before 100 °C, during which a weight fluctuation appears at about 77.0 °C. Accordingly, three endothermic peaks appear in DSC curve before 100 °C. An unexpected exothermic peak happens at 176.5 °C. Repeated STA tests were conducted considering the complex chemical composition and individual differences of EVM. Results indicate some general characterizations: the desorption process mainly happens before 100 °C, and can be divided into two or three phases. An exothermic peak emerges after 100 °C and is possibly initiated by the complex adherence force between adsorbed water and EVM.

In the TGA curve of LiCl·H_2O, two plateaus are observed, which means the formation of LiCl·H_2O and LiCl, respectively, according to weight calculation based on molar mass of LiCl and H_2O. The first plateau indicates that LiCl·H_2O deliquesces during the very short process of both weight measurement

and transfer to STA instrument. Due to the highly hydroscopic nature of LiCl·H_2O, its deliquescence can hardly be avoided. The red dotted line in the TGA curve represents the formation of LiCl·H_2O, namely the beginning of the dehydration reaction of LiCl·H_2O. Based on analysis of TGA/DSC curves, the process of free water loss has no direct connection with the dehydration reaction of LiCl·H_2O. The dehydration reaction of LiCl·H_2O is shown as follows, where the reaction heat is calculated based on the endothermic peak related to the desorption reaction:

$$\begin{gathered} LiCl \cdot H_2O\,(s) + HEAT \rightarrow LiCl\,(s) + H_2O\,(g)\,; \\ \Delta h_r = +63.95\ kJ/mol \end{gathered} \tag{3}$$

For all the EVM/LiCl sorbents, total water uptake acquired from TGA curve is almost the same as the result of sorption kinetics despite the tiny difference of water uptake caused by individual differences of composite sorbents. Accordingly, similar subtle difference in mass concentration between LiCl solution and the sorption kinetics results also exists. An obvious weight plateau is observed in the final stage of TGA curve, which means the formation of LiCl. Water uptake related to the formation of LiCl·H_2O is calculated by following formula:

$$x_{\mathrm{ad,LiCl}} = \eta \cdot x_{\mathrm{LiCl}}\,(g/g\ sorbent) \tag{4}$$

where x_{LiCl} is chemical sorption capacity of LiCl, 0.42 g/g LiCl.

The formation of LiCl·H_2O is showed on TGA curves by a red dotted line. Ignoring the negligible part of EVM, the desorption process of EVM/LiCl composite sorbents is divided into two processes:

Process 1:

$$(EVM + LiCl\ Solution) + HEAT \rightarrow (EVM + LiCl \cdot H_2O)\,(s) + nH_2O\,(g) \tag{5}$$

Process 2:

$$(EVM + LiCl \cdot H_2O)\,(s) + HEAT \rightarrow (EVM + LiCl)\,(s) + H_2O\,(g) \tag{6}$$

Only one desorption peak occurs in the DSC curve during the whole desorption process, identifying no distinct boundary between the desorption processes above. However, a turning point appears in the temperature representing the end of process 1, after which the slope of the DSC curve has an apparent change. Combining the mass calculation and this slope difference, processes 1 and 2 are demonstrated as different desorption stages. As a reversible process to the desorption process, the sorption of EVM/LiCl sorbents is composed of three stages: water adsorption of EVM, water adsorption of LiCl crystal, and liquid–gas absorption of LiCl solution. As soon as the dry EVM/LiCl sorbents get in contact with water vapor, EVM adsorbs a small amount of water vapor and reaches sorption equilibrium quickly. Meanwhile, LiCl in the pores gradually adsorbs water vapor and LiCl·H_2O is generated through a hydration reaction. After that, LiCl·H_2O crystal continues absorbing water, and LiCl solution is formed in consequence.

For EVM/LiCl sorbents, starting temperature of desorption peaks is almost the same, while the width of peaks increases with enhanced salt content. This phenomenon declares that the obstacle of mass transfer and heat conductivity is strengthened when a larger quantity of salt is embedded into EVM. Peak value of LiCl·H_2O is 101.3 °C, which is only slightly higher than 100 °C. Considering that the practical reaction temperature is lower than peak value, since the STA test is conducted at a rising temperature, the dehydration reaction of LiCl·H_2O is believed to happen below 100 °C. Peak values of EVMLiCl5, EVMLiCl10, and EVMLiCl20 are 64.7 °C, 74.7 °C, and 90.0 °C, respectively, which are entirely below 100 °C. In general, LiCl can be finally formed in EVM/LiCl sorbents when employing low-temperature heat below 100 °C the as desorption energy resource.

3.4. Theoretical Evaluation of Sorption Performance

To analyze sorption performance and energy storage potential for a TES system, further theoretical calculation and analyses are implemented. Water uptake of EVM/LiCl composite sorbents is divided into three portions: physical adsorption of EVM ($x_{ad,EVM}$), chemical adsorption of LiCl crystal ($x_{ad,LiCl}$), and liquid-gas absorption of LiCl solution ($x_{ab,LiCl}$). Total water uptake x_{cs} is obtained from the TGA curve, $x_{ad,LiCl}$ is calculated through Equation (3), and $x_{ad,EVM}$ and $x_{ab,LiCl}$ are calculated using the following equations:

$$x_{ad,EVM} = (1 - \eta) \cdot x_{EVM} \, (g/g \; sorbent) \tag{7}$$

$$x_{ab,LiCl} = x_{cs} - x_{ad,EVM} - x_{ad,LiCl} \, (g/g \; sorbent) \tag{8}$$

Figure 6 shows the sorption performances of EVM, LiCl·H_2O, and EVM/LiCl sorbents. When taking the hydration reaction alone into consideration, the total water uptake of LiCl is 0.42 g/g, which is smaller than those of all the composite sorbents. The value of x_{cs} increases from 0.50 g/g to 1.41 g/g with increasing salt content. EVMLiCl20 reaches the largest water uptake of 1.41 g/g, which is 3.4 times larger than that of LiCl·H_2O. For EVM/LiCl sorbents, values of $x_{ad,LiCl}$ and $x_{ab,LiCl}$ increase with the enhanced salt concentration. Adsorption of EVM is responsible for 1.9%–6.8% of total water sorption, while water adsorbed by LiCl contributes only 9.8%–10.2%. 83.0%–88.3% of the total water uptake is introduced by liquid-gas absorption of LiCl solution. Moreover, the ratio of $x_{ab,LiCl}/x_{ad,LiCl}$ increases from 8.2 to 9.0 with increasing salt content, which indicates that larger pore volume of EVM contributes to LiCl solution preservation.

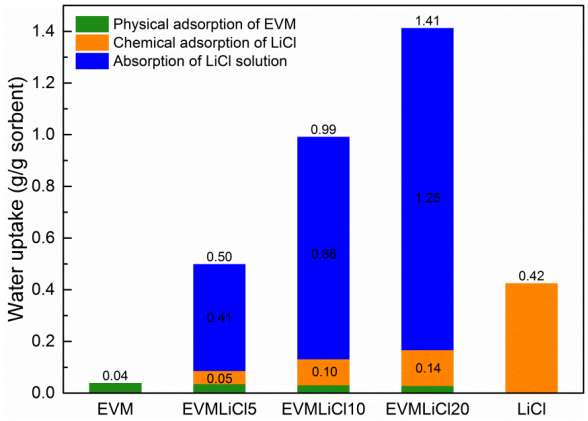

Figure 6. Sorption performances of EVM, LiCl·H_2O, and EVM/LiCl sorbents.

3.5. Theoretical Evaluation of Energy Storage Density

Mass energy storage density (q_m) can be approximately assesses by desorption heat obtained from DSC curves. Sorption heat in three parts of the whole sorption process ($q_{ad,EVM}$, $q_{ad,LiCl}$, and $q_{ab,LiCl}$) is analyzed, whose calculation equations are listed as follows:

$$q_{ad,EVM} = (1 - \eta) \cdot q_{m,EVM} \, (kWh/kg \; sorbent) \tag{9}$$

$$q_{ad,LiCl} = \eta \cdot q_{m,LiCl} \, (kWh/kg \; sorbent) \tag{10}$$

$$q_{ab,LiCl} = q_{m,cs} - q_{ad,EVM} - q_{ad,LiCl} \, (kWh/kg \; sorbent) \tag{11}$$

where $q_{m,LiCl}$ is hydration reaction heat gained from the DSC curve in Figure 5b, $q_{m,EVM}$ is adsorption heat of EVM obtained from the DSC curve in Figure 5a, and $q_{m,LiCl}$ is total sorption heat of composite sorbents acquired from Figure 5c–e.

Figure 7 shows the mass energy storage density of EVM, LiCl·H_2O, and EVM/LiCl sorbents. $q_{m,EVM}$ is merely 0.02 kWh/kg, while that of LiCl·H_2O is 0.42 kWh/kg. Mass energy storage density

increases with greater salt content, and those of EVMLiCl10 and EVMLiCl20 exceed that of LiCl·H_2O. EVMLiCl20 can reach a mass energy storage density of 1.21 kWh/kg, which is 2.9 times higher than that of LiCl·H_2O. $q_{ad,EVM}$ and $q_{ab,LiCl}$ also increase with greater salt content. Absorption heat contributes 77.4%–87.5% of mass energy storage density, while adsorption heat of LiCl contributes 11.3%–16.1%. Compared with the sorption process without solution absorption, the addition of the absorption process extensively improves $q_{m,cs}$ by 2.42–5.97 times, which is more evident with larger salt content.

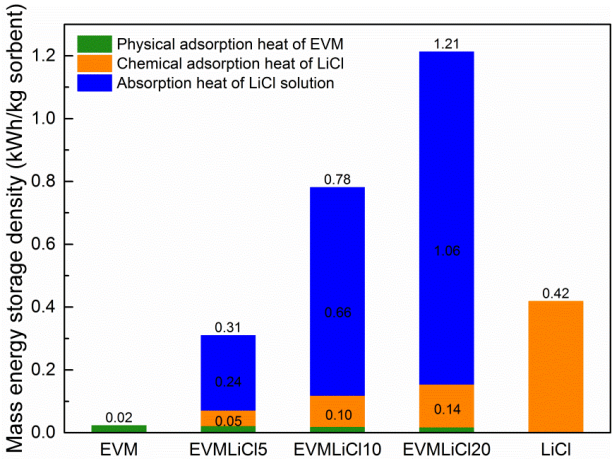

Figure 7. Mass energy storage density of EVM, LiCl·H_2O, and EVM/LiCl sorbents.

Volume energy storage density (q_v) is another key parameter for the realization of a compact TES system. The calculation equation of q_v is as follows:

$$q_v = \rho \cdot q_m \left(kWh/m^3\right) \tag{12}$$

where ρ is bulk density of sorbent listed in Table 1.

Calculation results are shown in Figure 8. Volume energy storage density of EVM is only 2.96 kWh/m^3. The theoretical volume energy storage density of LiCl·H_2O can reach 745.94 kWh/m^3. However, this high theoretical value is usually confined by serious mass and heat transfer restrictions. Moreover, the reliability and repeatability are further hindered due to the swelling and agglomerate phenomenon of salt. Surprisingly, EVM/LiCl composite sorbents suffer no such problems. The value of q_v of EVM/LiCl sorbents increases with greater salt concentration, and the largest value of 167.04 kWh/m^3 is acquired by EVMLiCl20.

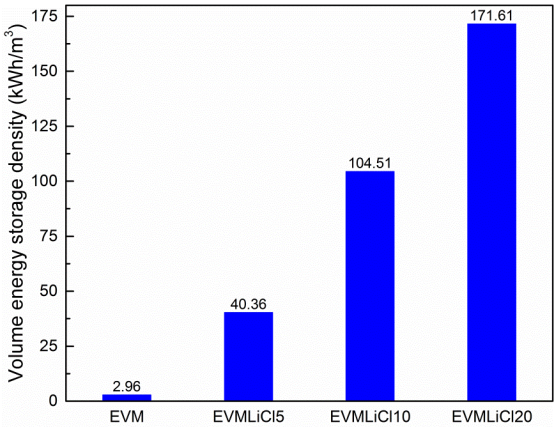

Figure 8. Volume energy storage density of EVM and EVM/LiCl sorbents.

Sorption heat is originated from the interaction force between sorbent and water vapor, and a common relation is usually followed. Reaction enthalpy of whole desorption process ($\Delta h_{r,w}$) is a vital parameter. For composite sorbents, sorption reaction enthalpy is composed of three parts: physical adsorption enthalpy of EVM ($\Delta h_{ad,EVM}$), chemical adsorption enthalpy of LiCl ($\Delta h_{ad,LiCl}$), and liquid–gas absorption of LiCl solution ($\Delta h_{ab,LiCl}$). $\Delta h_{ad,EVM}$ and $\Delta h_{ad,LiCl}$ share the same value with $\Delta h_{r,w}$ of pure EVM and pure LiCl, accordingly. The value of $\Delta h_{ab,LiCl}$ is influenced by salt content and pore structure of composite sorbents. They are calculated using the following equations:

$$\Delta h_{r,w} = \frac{3.6 q_m M_{H_2O}}{x_w} \ (kJ/mol) \tag{13}$$

$$\Delta h_{ad,EVM} = \frac{3.6 q_{EVM} M_{H_2O}}{x_{EVM}} \ (kJ/mol) \tag{14}$$

$$\Delta h_{ad,LiCl} = \frac{3.6 q_{m,LiCl} M_{H_2O}}{x_{LiCl}} \ (kJ/mol) \tag{15}$$

$$\Delta h_{ab,LiCl} = \frac{3.6 q_{ab,salt} M_{H_2O}}{x_{ab,salt}} \ (kJ/mol) \tag{16}$$

Figure 9 shows the calculation results. Generally, the desorption heat for losing one mole water ranges from 38 to 64 kJ, which can be a rough calculation criterion to assess desorption heat on the basis of water uptake. Among all the sorbents, EVM has the lowest $\Delta h_{r,w}$ of 38.90 kJ/mol while LiCl·H_2O has the largest $\Delta h_{r,w}$ of 63.95 kJ/mol, and the value of $\Delta h_{r,w}$ for EVM/LiCl sorbents is modest. Thus, the chemical sorption process is demonstrated to release more heat than the physical sorption process. For EVM/LiCl sorbents, the value of $\Delta h_{r,w}$ increases with increased salt content, and the differences between composite sorbents lay in different values of $\Delta h_{ab,LiCl}$. As mentioned above, mass concentration of LiCl solution held in EVM pores is almost the same for three composite sorbents, but the value of $\Delta h_{ab,salt}$ increases from 37.59 to 55.19 kJ/mol with increasing salt content. For composite sorbents, LiCl solution is confined in numerous pores. Adhesive forces between LiCl solution and the surface of pores, mass transfer resistance, and the concentration heat of LiCl are three forces influencing $\Delta h_{ab,salt}$. The former two kinds of forces increase with increased salt content, which eventually contributes to the enhancement of $\Delta h_{ab,salt}$.

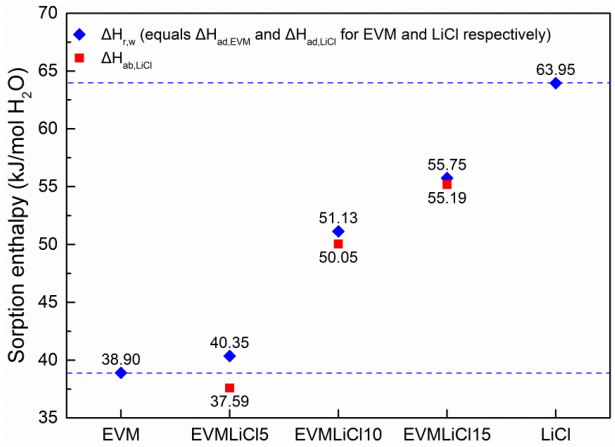

Figure 9. Enthalpy of gross sorption process and three sectional sorption processes of composite sorbents.

4. Conclusions

This paper aims to develop novel composite sorbents employing EVM, which has a macroporous structure, as host matrix rather than using traditional mesoporous materials (i.e., silica gel and zeolite).

Highly hydroscopic salt LiCl was chosen as the inserting component to fully take advantage of the large volume of EVM. To study the sorption performance and evaluate the potential of EVM/LiCl composites for low-temperature (<100 °C) heat storage, several experiments and theoretical calculation were implemented. Basically, three conclusions are drawn:

1. Sorption process of EVM/LiCl composite sorbents is composed of three parts: physical adsorption of EVM, chemical adsorption of LiCl crystal, and liquid-gas absorption of LiCl solution. The salt content threshold for composite sorbents is 32.60%, beyond which solution leakage may appear. Not all of the pore volume of EVM can be utilized owing to some inaccessible volumes produced by the block of LiCl crystals and the stack of LiCl crystals.
2. Compared with pure LiCl, sorption kinetics and thermochemical performance of LiCl embedded into EVM present better performances: water uptake is increased as lower mass concentration LiCl solution is formed in EVM pores; desorption reaction enthalpy of LiCl solution is improved due to the contribution of adhesive forces between LiCl solution and the surface of pores and mass transfer resistance.
3. Water uptake, mass energy storage density, and volume energy storage density increase with salt content. Water absorbed by LiCl solution contributes 83.0%–88.3% of total water uptake, and accordingly the sorption heat released in this process takes 77.4%–87.5% of the mass energy storage density. The desorption heat for losing one mole water ranges from 38 to 64 kJ. EVMLiCl20 was selected as the optimal composite sorbent, with water uptake of 1.41 g/g, mass energy storage density of 1.21 kWh/kg, and volume energy storage density of 171.61 kWh/m^3.

In general, EVM is demonstrated as a kind of excellent macroporous matrix for increasing the water uptake of CSPMs. By taking advantage of salt deliquescence to a large extent, EVM/LiCl composite sorbents present promising properties for low-temperature TES systems.

Acknowledgments: This work was supported by the National Natural Science Funds for Excellent Young Scholar of China under the contract No. 51522604 and the Foundation for Innovative Research Groups of the National Natural Science Foundation of China under the contract No. 51521004.

Author Contributions: Yannan Zhang and Yanjie Zhao conceived and designed the experiments; Yannan Zhang performed the experiments; Yannan Zhang and Tingxian Li analyzed the data; Ruzhu Wang contributed reagents/materials/analysis tools; Yannan Zhang wrote the paper.

Conflicts of Interest: The authors declare no conflict of interest.

Abbreviations

The following abbreviations are used in this manuscript:

EVM	expanded vermiculite
TES	thermal energy storage
CSPM	salt inside porous matrix
RH	relative humidity
DRH	deliquescence relative humidity
PCM	phase change material

Nomenclature

w	mass concentration of LiCl solution in EVM pores, %
v_s	volume of the LiCl solution formed in EVM pores, cm^3/g
x	water uptake, g/g
q_m	mass energy storage density of sorbent, kWh/kg
q	sorption heat of each part of the whole sorption process, kWh/kg
q_v	volume energy storage density, kWh/m^3

Greek symbols

η	mass concentration of LiCl in composite sorbent, %
ρ	bulk density, kg/m^3
$\Delta h_{r,w}$	reaction enthalpy for losing per mole water of the whole sorption process, kJ/mol
Δh	reaction enthalpy for losing per mole water of each part of the whole sorption process, kJ/mol

Subscripts

EVM	raw expanded vermiculite
LiCl	pure lithium chloride
cs	EVM/LiCl composite sorbent
ad,EVM	physical adsorption of EVM for EVM/LiCl composite sorbents
ad,LiCl	chemical adsorption of LiCl crystals in EVM/LiCl composite sorbents
ab,LiCl	liquid-gas absorption of LiCl solution for EVM/LiCl composite sorbents

References

1. Aydin, D.; Casey, S.P.; Riffat, S. The latest advancements on thermochemical heat storage systems. *Renew. Sustain. Energy Rev.* **2015**, *41*, 356–367. [CrossRef]
2. Liu, H.; Nagano, K.; Togawa, J. A composite material made of mesoporous siliceous shale impregnated with lithium chloride for an open sorption thermal energy storage system. *Sol. Energy* **2015**, *111*, 186–200. [CrossRef]
3. Nakabayashi, S.; Nagano, K.; Nakamura, M.; Togawa, J.; Kurokawa, A. Improvement of water vapor adsorption ability of natural mesoporous material by impregnating with chloride salts for development of a new desiccant filter. *Adsorption* **2011**, *17*, 675–686. [CrossRef]
4. Posern, K.; Kaps, C. Calorimetric studies of thermochemical heat storage materials based on mixtures of $MgSO_4$ and $MgCl_2$. *Thermochim. Acta* **2010**, *502*, 73–76. [CrossRef]
5. Michel, B.; Mazet, N.; Mauran, S.; Stitou, D.; Xu, J. Thermochemical process for seasonal storage of solar energy: Characterization and modeling of a high density reactive bed. *Energy* **2012**, *47*, 553–563. [CrossRef]
6. Deshmukh, H.; Maiya, M.P.; Murthy, S. Study of sorption based energy storage system with silica gel for heating application. *Appl. Therm. Eng.* **2016**. [CrossRef]
7. Frazzica, A.; Sapienza, A.; Freni, A. Novel experimental methodology for the characterization of thermodynamic performance of advanced working pairs for adsorptive heat transformers. *Appl. Therm. Eng.* **2014**, *72*, 229–236. [CrossRef]
8. Gong, L.X.; Wang, R.Z.; Xia, Z.Z.; Chen, C.J. Adsorption equilibrium of water on a composite adsorbent employing lithium chloride in silica gel. *J. Chem. Eng. Data* **2010**, *55*, 2920–2923. [CrossRef]
9. Yu, N.; Wang, R.Z.; Lu, Z.S.; Wang, L.W. Development and characterization of silica gel-LiCl composite sorbents for thermal energy storage. *Chem. Eng. Sci.* **2014**, *111*, 73–84. [CrossRef]
10. Zheng, X.; Ge, T.S.; Wang, R.Z.; Hu, L.M. Performance study of composite silica gels with different pore sizes and different impregnating hygroscopic salts. *Chem. Eng. Sci.* **2014**, *120*, 1–9. [CrossRef]
11. Whiting, G.T.; Grondin, D.; Stosic, D.; Bennici, S.; Auroux, A. Zeolite-$MgCl_2$ composites as potential long-term heat storage materials: Influence of zeolite properties on heats of water sorption. *Sol. Energy Mater. Sol. Cells* **2014**, *128*, 289–295. [CrossRef]
12. Casey, S.P.; Elvins, J.; Riffat, S.; Robinson, A. Salt impregnated desiccant matrices for open thermochemical energy storage—Selection, synthesis and characterisation of candidate materials. *Energy Build.* **2014**, *84*, 412–425. [CrossRef]
13. Veselovskaya, J.V.; Tokarev, M.M.; Grekova, A.D.; Gordeeva, L.G. Novel ammonia sorbents "porous matrix modified by active salt" for adsorptive heat transformation: 6. The ways of adsorption dynamics enhancement. *Appl. Therm. Eng.* **2012**, *37*, 87–94. [CrossRef]
14. Aristov, Y.I.; Restuccia, G.; Tokarev, M.M.; Buerger, H.D.; Freni, A. Selective water sorbents for multiple applications. 11. $CaCl_2$ confined to expanded vermiculite. *React. Kinet. Catal. Lett.* **2000**, *71*, 377–384. [CrossRef]
15. Shkatulov, A.; Ryu, J.; Kato, Y.; Aristov, Y. Composite material "$Mg(OH)_2$/vermiculite": A promising new candidate for storage of middle temperature heat. *Energy* **2012**, *44*, 1028–1034. [CrossRef]

16. Sapienza, A.; Glaznev, I.S.; Santamaria, S.; Freni, A.; Aristov, Y.I. Adsorption chilling driven by low temperature heat: New adsorbent and cycle optimization. *Appl. Therm. Eng.* **2012**, *32*, 141–146. [CrossRef]
17. Grekova, A.D.; Veselovskaya, J.V.; Tokarev, M.M.; Gordeeva, L.G. Novel ammonia sorbents "porous matrix modified by active salt" for adsorptive heat transformation: 5. Designing the composite adsorbent for ice makers. *Appl. Therm. Eng.* **2012**, *37*, 80–86. [CrossRef]
18. Veselovskaya, J.V.; Critoph, R.E.; Thorpe, R.N.; Metcalf, S.; Tokarev, M.M.; Aristov, Y.I. Novel ammonia sorbents "porous matrix modified by active salt" for adsorptive heat transformation: 3. Testing of "$BaCl_2$/vermiculite" composite in a lab-scale adsorption chiller. *Appl. Therm. Eng.* **2010**, *30*, 1188–1192. [CrossRef]
19. Guan, W.M.; Li, J.H.; Qian, T.T.; Wang, X.; Deng, Y. Preparation of paraffin/expanded vermiculite with enhanced thermal conductivity by implanting network carbon in vermiculite layers. *Chem. Eng. J.* **2015**, *277*, 56–63. [CrossRef]
20. Kheradmand, M.; Castro-Gomes, J.; Azenha, M.; Silva, P.D.; De Aguiar, J.L.B.; Zoorob, S.E. Assessing the feasibility of impregnating phase change materials in lightweight aggregate for development of thermal energy storage systems. *Constr. Build. Mater.* **2015**, *89*, 48–59. [CrossRef]
21. Gordeeva, L.G.; Aristov, Y.I. Composite sorbent of methanol "LiCl in mesoporous silica gel" for adsorption cooling: Dynamic optimization. *Energy* **2011**, *36*, 1273–1279. [CrossRef]
22. Yu, N.; Wang, R.Z.; Wang, L.W. Theoretical and experimental investigation of a closed sorption thermal storage prototype using LiCl/water. *Energy* **2015**, *93*, 1523–1534. [CrossRef]
23. Grekova, A.; Gordeeva, L.; Aristov, Y. Composite sorbents "Li/Ca halogenides inside multi-wall carbon nano-tubes" for thermal energy storage. *Sol. Energy Mater. Sol. Cells* **2016**, *155*, 176–183. [CrossRef]
24. Conde, M.R. Properties of aqueous solutions of lithium and calcium chlorides: Formulations for use in air conditioning equipment design. *Int. J. Therm. Sci.* **2004**, *43*, 367–382. [CrossRef]